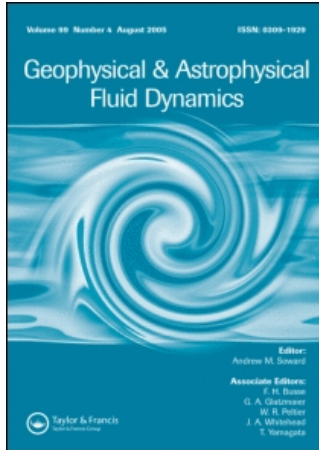


This article was downloaded by:[The University of Manchester]
On: 23 April 2008
Access Details: [subscription number 773564140]
Publisher: Taylor & Francis
Informa Ltd Registered in England and Wales Registered Number: 1072954
Registered office: Mortimer House, 37-41 Mortimer Street, London W1T 3JH, UK



Geophysical & Astrophysical Fluid Dynamics

Publication details, including instructions for authors and subscription information:
<http://www.informaworld.com/smpp/title-content=t713642804>

The scattering of Rossby waves from finite abrupt topography

G. W. Owen^a; A. J. Willmott^a; I. D. Abrahams^b; H. Mansley^a

^a Department of Mathematics, Keele University, Staffordshire, ST5 5BG, UK

^b Department of Mathematics, University of Manchester, Manchester, M13 9PL, UK

Online Publication Date: 01 June 2005

To cite this Article: Owen, G. W., Willmott, A. J., Abrahams, I. D. and Mansley, H. (2005) 'The scattering of Rossby waves from finite abrupt topography', Geophysical & Astrophysical Fluid Dynamics, 99:3, 219 - 239

To link to this article: DOI: 10.1080/03091920500087690

URL: <http://dx.doi.org/10.1080/03091920500087690>

PLEASE SCROLL DOWN FOR ARTICLE

Full terms and conditions of use: <http://www.informaworld.com/terms-and-conditions-of-access.pdf>

This article may be used for research, teaching and private study purposes. Any substantial or systematic reproduction, re-distribution, re-selling, loan or sub-licensing, systematic supply or distribution in any form to anyone is expressly forbidden.

The publisher does not give any warranty express or implied or make any representation that the contents will be complete or accurate or up to date. The accuracy of any instructions, formulae and drug doses should be independently verified with primary sources. The publisher shall not be liable for any loss, actions, claims, proceedings, demand or costs or damages whatsoever or howsoever caused arising directly or indirectly in connection with or arising out of the use of this material.

The scattering of Rossby waves from finite abrupt topography

G. W. OWEN^{†*}, A. J. WILLMOTT[†], I. D. ABRAHAMS[‡] and H. MANSLEY[†]

[†]Department of Mathematics, Keele University, Keele, Staffordshire, ST5 5BG, UK

[‡]Department of Mathematics, University of Manchester,
Oxford Road, Manchester, M13 9PL, UK

(Received 25 November 2004; in final form 14 February 2005)

The scattering of first mode linear baroclinic Rossby waves by a top-hat ridge in a continuously stratified ocean, with Brunt-Väisälä frequency that decays exponentially with depth below a surface mixed layer, is the subject of this study. A numerical mode matching technique is used to calculate the transmission coefficients for the propagating modes over the ridge. It is found that the scattered field depends crucially upon the stratification. For example, when the majority of the density variation is confined to a thin thermocline, corresponding to a small e-folding scale, γ^{-1} , for the Brunt-Väisälä frequency, a large amount of the incident wave energy is reflected by a small amplitude ridge. Appreciable energy conversion between the propagating barotropic and baroclinic modes takes place in this case. An asymptotic analysis for a small amplitude ridge is presented that confirms these numerical results. In the limit $\gamma^{-1} \rightarrow 0$, it is demonstrated that the scattered field in the continuously stratified ocean model differs markedly from the two-layer solution. The latter does not exhibit appreciable reflection of the incident wave energy for a small amplitude ridge. In conclusion, the application of a two-layer ocean model to describe Rossby wave scattering by ridges in place of a continuously stratified model cannot be recommended.

Keywords: Rossby wave; Continuous stratification; Abrupt topography

1. Introduction

This article extends the study of Owen *et al.* (2002), which considered the scattering of baroclinic Rossby waves by abrupt topography in a continuously stratified ocean. In that paper, the analysis was limited to an ocean with constant buoyancy frequency and topography in the form of a vertical submerged barrier of negligible width. It was shown that even relatively small amplitude topography generates an appreciable magnitude of wave reflection and energy conversion between the propagating modes.

*Corresponding author. Email: g.w.owen@maths.keele.ac.uk

In the present article, several physically realistic elements are added to the model discussed in Owen *et al.* (2002). First a vertical barrier of non-zero finite width (i.e. a top-hat ridge in side elevation) is introduced. Additionally, the scattering problem is generalized to include an exponential profile for the buoyancy frequency, typical of that observed in the mid-ocean (Emery *et al.* 1984). A solution scheme for a wide range of parameter values is presented in addition to an asymptotic approach for the case of topography of small height. Comparisons are made with results from layered models, such as those considered in Wang and Koblinsky (1994).

The important rôle played by Rossby waves in the long term adjustment of the ocean has been long known, and the advent of accurate satellite altimetry has led to increased knowledge of, and a renewed interest in, the dynamics of large scale planetary Rossby waves in the Earth's oceans. The signature of slow baroclinic waves has been extracted from the altimetry of the TOPEX/Poseidon satellite (e.g. Chelton and Schlax 1996) and the Along Track Scanning Radiometer (ATSR) (e.g. Hill *et al.* 2000), and this has given us a synoptic view of their propagation characteristics.

2. Mathematical formulation

2.1. Equations of motion and geometry

We shall consider a model which consists of a Boussinesq fluid of constant reference density ρ_* , with continuous vertical stratification specified by the Brunt-Väisälä frequency

$$N^2(z) = -\frac{g}{\rho_*} \frac{d\rho}{dz}, \quad (1)$$

where g is the acceleration due to gravity, ρ is the density field and z is the vertical coordinate. We commence the investigation by considering a flat bottomed ocean which contains an abrupt change in depth along an infinite line inclined at an arbitrary angle, θ , to the E-W axis, as shown in figure 1 and 2. We shall use the primed variables, x', y' , to denote horizontal coordinates aligned with longitude and latitude respectively, and the unprimed variables, x, y , to denote coordinates along and perpendicular to the escarpment, which lies at $y=0$ (see figure 1). The coordinate orthogonal to both the primed and unprimed variables, z , points vertically upwards.

We shall assume that the ocean is at rest, except for low-frequency (i.e. sub-inertial) oscillations in the form of planetary Rossby waves. We shall model the meridional variation of the Coriolis parameter, f , as a mid-latitude β -plane and thus write

$$f(y') = f_0 + \beta y', \quad (2)$$

where $f_0 \gg \beta y'$ over the entire range of interest. In this case, the velocity field, \mathbf{u} , of the fluid is completely determined by a quasi-geostrophic (QG) streamfunction, $\psi(x, y, z, t)$, in the form

$$\mathbf{u} = \left(\frac{\partial \psi}{\partial y}, -\frac{\partial \psi}{\partial x}, -\frac{f_0}{N^2(z)} \frac{\partial^2 \psi}{\partial z \partial t} \right), \quad (3)$$

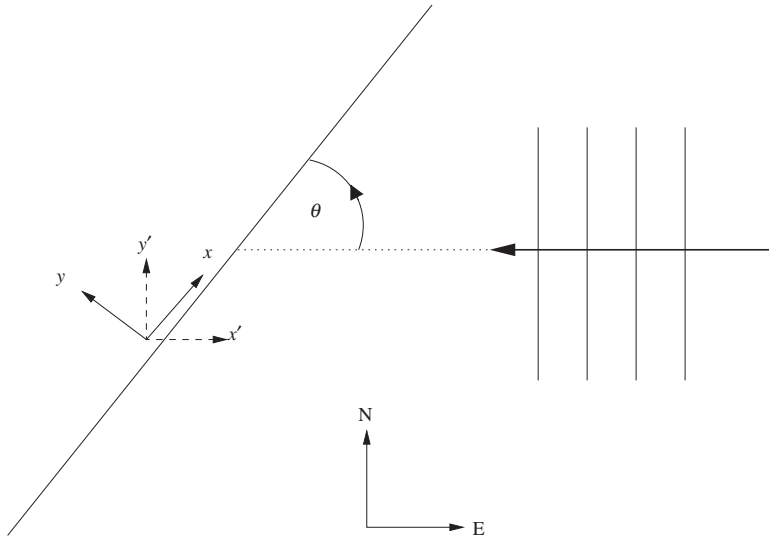


Figure 1. Schematic of horizontal geometry.

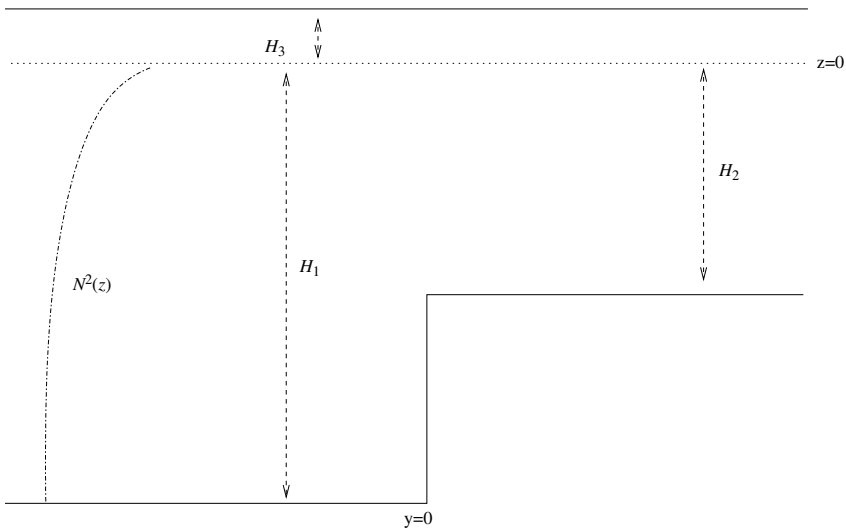


Figure 2. Vertical schematic of escarpment, showing geometry and exponential stratification. Note that the origin $z=0$ is taken, for convenience, at the bottom of the mixed layer and $H_1 > H_2 > 0$.

where the velocity components are taken in the directions of the unprimed coordinates. It may be shown (see Pedlosky 1979) that such a streamfunction satisfies the linear Rossby wave equation,

$$\frac{\partial}{\partial t} \left\{ \nabla_H^2 \psi + f_0^2 \frac{\partial}{\partial z} \left[\frac{1}{N^2(z)} \frac{\partial \psi}{\partial z} \right] \right\} + \beta \left\{ \cos \theta \frac{\partial \psi}{\partial x} - \sin \theta \frac{\partial \psi}{\partial y} \right\} = 0, \quad (4)$$

where ∇_H^2 is the horizontal Laplacian, containing no derivatives in z . Writing the streamfunction in the form

$$\psi = \exp(ikx + ily - i\omega t)\Gamma(z), \quad (5)$$

where $\mathbf{k} = (k, l)$ is a constant wavenumber vector and ω a constant angular wave frequency, equation (4) is separable, provided that the undisturbed fluid depth is piecewise constant. Therefore, we may express solutions of equation (4) in terms of vertical normal modes, where each mode is a solution of the Sturm–Liouville eigenvalue equation

$$\frac{d}{dz} \left[\frac{1}{N^2(z)} \frac{d\Gamma_n}{dz} \right] + \frac{1}{gh_n} \Gamma_n(z) = 0, \quad (6)$$

with $d\Gamma_n/dz = 0$, at the horizontal boundaries. At $z = H_1$ or $z = H_2$, depending upon the domain (see figure 2, with $H_1 > H_2$) this boundary condition represents the impermeable ocean bottom. At the surface, $z = H_3$, it represents a rigid lid boundary condition. The eigenvalue h_n is the equivalent depth of the n th vertical mode. Upon substitution into equation (4) we obtain the dispersion relation

$$\omega = \frac{\beta(l \sin \theta - k \cos \theta)}{k^2 + l^2 + f_0^2/gh_n}. \quad (7)$$

Clearly, the dependence of each h_n on the fluid depth means we have two distinct sets of eigenvalues and vertical modes, one in the deep and one in the shallow regions. We shall denote the two families of complete, orthonormal eigenfunctions by $\Gamma_n(z)$ and $\gamma_n(z)$ respectively and the associated pairs of roots of the dispersion relation (7), for fixed k and ω , by (l_n, s_n) in the deep region and (\hat{l}_n, \hat{s}_n) in the shallow region. Here the wavenumbers l_n and \hat{l}_n correspond to the long (westward) waves, while s, \hat{s}_n correspond to the short (eastward) waves in each region.

We may write the QG streamfunction in terms of the sum of such vertical normal modes. In the region $y > 0$ we have only a transmitted wave field, whereas in $y < 0$ we take a single long (westward) incident mode of unit amplitude and a reflected wave field, with both reflected and transmitted fields satisfying the Sommerfeld radiation condition that the group velocity be away from the topography. Suppressing the $\exp(ikx - i\omega t)$ dependence for ease of presentation, the streamfunction is given by

$$\psi(y, z) = \begin{cases} \sum_{j=0}^{\infty} T_j e^{i\hat{l}_j y} \gamma_j(z), & y > 0, \\ \left[\sum_{j=0}^{\infty} R_j e^{is_j y} \Gamma_j(z) - e^{is_1 y} \Gamma_1(z) \right] + e^{i\hat{l}_1 y} \Gamma_1(z), & y < 0, \end{cases} \quad (8)$$

where T_i and R_i are the unknown transmission and reflection coefficients. The bracketed term in equation (8) represents the reflected wave field, with an additional reflected mode of unit amplitude included purely for algebraic convenience.

We shall consider the flow over two distinct but related idealized forms of the topography. The first, shown in figure 2, is a flat-bottomed ocean with a single abrupt change of depth along $y=0$, which represents a sharp escarpment or the edge of the continental shelf. The second is a ‘‘top hat’’ ridge of finite width, say

$-l < y < l$, which may be thought of as representing an abrupt ridge system, such as the mid-Atlantic ridge or the Hawaiian range. The latter will be addressed in section 4 when numerical results are offered, but before then we focus on a single escarpment lying along $y = 0$.

The system is closed by the vertical boundary and continuity conditions. The modal structure guarantees that there is no normal flow at the ocean floor or the “rigid-lid” surface. We now insist that there is no flow through the vertical face of the escarpment and that both components of the horizontal velocity field are continuous above the face. Therefore, on the topography’s vertical face we have

$$\psi = 0, \quad \text{on } y = 0, \quad -H_1 < z < -H_2. \tag{9}$$

and

$$\left[\frac{\partial \psi}{\partial y} \right] = \left[\frac{\partial \psi}{\partial x} \right] = 0 \quad \text{on } -H_2 < z < 0, \tag{10}$$

where $[f]$ denotes the jump in f . To determine the reflected and transmitted wavefields, it is necessary to find the scattering coefficients R_j and T_j . We do this using a modified version of the method employed in Owen *et al.* (2002), which is outlined below.

3. Method of solution

3.1. General method

To proceed, we first recast the boundary conditions in equation (9) and (10) in terms of the scattering coefficients by multiplying each by $\Gamma_i(z)$ and integrating in the vertical direction over their respective ranges of validity. Upon integrating equation (9), and using the orthonormality of the modes we obtain

$$0 = \int_{-H_1}^{-H_2} \psi(0, z) \Gamma_i(z) dz = \sum_{j=0}^{\infty} \left\{ \int_{-H_1}^{-H_2} \Gamma_i(z) \Gamma_j(z) dz \right\} R_j = \sum_{j=0}^{\infty} (\delta_{ij} - C_{ij}) R_j, \tag{11}$$

where δ_{ij} is the Kronecker delta and the infinite symmetric matrix \mathbf{C} is defined by

$$C_{ij} = \int_{-H_2}^{H_3} \Gamma_i(z) \Gamma_j(z) dz. \tag{12}$$

Note that z is measured vertically upwards from a distance H_3 below the free surface. As discussed in Owen *et al.* (2002), after truncation as an $N \times N$ matrix, the eigenvectors of \mathbf{C} will be partitioned into a set of M , denoted $\mathbf{v}_1, \mathbf{v}_2, \dots, \mathbf{v}_M$, with associated eigenvalue approximately equal to unity, and $N - M$ eigenvectors with associated eigenvalue approximately equal to zero. Equation (11) may then be rewritten in the algebraic form,

$$(\mathbf{I} - \mathbf{C}) \mathbf{R} = 0, \tag{13}$$

where \mathbf{I} is the $N \times N$ identity matrix. From equation (13) it may be seen that the $N \times 1$ vector \mathbf{R} of reflection coefficients must be a linear combination of the eigenvectors \mathbf{v}_i , i.e.

$$\mathbf{R} \simeq \sum_{i=1}^M \alpha_i \mathbf{v}_i. \quad (14)$$

The result of imposing the no normal flow condition on the escarpment face, then, is to reduce the number of unknowns from the N (the R_i), to M (the α_i). Integrating the continuity equations in (10) above the escarpment, we find

$$\sum_{i=0}^{\infty} T_i \left\{ \int_{-H_2}^0 \gamma_i(z) \Gamma_j(z) dz \right\} = \sum_{i=0}^{\infty} R_i \left\{ \int_{-H_2}^0 \Gamma_i(z) \Gamma_j(z) dz \right\}, \quad (15)$$

$$\begin{aligned} \sum_{i=0}^{\infty} T_i \hat{l}_i \left\{ \int_{-H_2}^0 \gamma_i(z) \Gamma_j(z) dz \right\} &= \sum_{i=0}^{\infty} R_i s_i \left\{ \int_{-H_2}^0 \Gamma_i(z) \Gamma_j(z) dz \right\} \\ &+ (l_1 - s_1) \int_{-H_2}^0 \Gamma_1(z) \Gamma_j(z) dz. \end{aligned} \quad (16)$$

We now define two $N \times M$ matrices, \mathbf{V} and \mathbf{G} , where \mathbf{V} has the vectors $\mathbf{v}_1, \dots, \mathbf{v}_M$ as columns and the elements of \mathbf{G} are given by

$$G_{ij} = \int_{-H_2}^{H_3} \Gamma_i(z) \gamma_j(z) dz. \quad (17)$$

Truncating the left hand sides of equations (15) and (16) at M terms, and their right hand sides at N terms we find

$$\mathbf{GT} = \mathbf{CR} = \mathbf{R} = \mathbf{V}\boldsymbol{\alpha}, \quad (18)$$

$$\mathbf{GLT} = \mathbf{CSR} + \mathbf{C}(\mathbf{L} - \mathbf{S}) = \mathbf{CSV}\boldsymbol{\alpha} + \mathbf{C}(\mathbf{L} - \mathbf{S})\mathbf{e}_1, \quad (19)$$

where \mathbf{S} and \mathbf{L} are $N \times N$ diagonal matrices with the s_i and l_i on the diagonals, respectively, $\hat{\mathbf{L}}$ is $M \times M$ with the \hat{l}_i on the diagonal and \mathbf{e}_1 is the column vector with a 1 in the second row and zeros elsewhere. Since \mathbf{C} is symmetric we know that the vectors \mathbf{v}_i are mutually orthogonal and so, without loss of generality, we may assume that

$$\mathbf{V}^T \mathbf{V} = \mathbf{I}, \quad (20)$$

where \mathbf{I} is the $M \times M$ identity matrix, and by construction it may be seen that

$$\mathbf{CV} = \mathbf{V} \quad \text{and} \quad \mathbf{V}^T \mathbf{C} = \mathbf{V}^T. \quad (21)$$

Pre-multiplying equation (18) by $\mathbf{V}^T \mathbf{S}$ and equation (19) by \mathbf{V}^T and eliminating $\boldsymbol{\alpha}$ we obtain the $M \times M$ matrix system

$$(\mathbf{V}^T \mathbf{GL} - \mathbf{V}^T \mathbf{SG})\mathbf{T} = \mathbf{V}^T (\mathbf{L} - \mathbf{S})\mathbf{e}_1. \quad (22)$$

This system is invertible, and hence can be used to find the M transmission coefficients. The reflection coefficients are then determined directly from equation (18).

3.2. Specific stratifications

3.2.1. Constant stratification. To check the integrity of the numerical procedure described in section 3.1, we again make the simplifying assumption that $N(z) = N_0$ is constant throughout the fluid, as in Owen *et al.* (2002). In this case the Sturm-Liouville eigenvalue equation (6) reduces to

$$\frac{d^2\Gamma_n}{dz^2} + \frac{N_0^2}{gh_n}\Gamma_n(z) = 0. \quad (23)$$

Thus, the equivalent depths in $y < 0$ are $gh_n = H_1^2 N_0^2 / n^2 \pi^2$ and the vertical eigenfunctions are given by

$$\Gamma_0 = \sqrt{\frac{1}{H_1}} \quad \text{and} \quad \Gamma_n = \sqrt{\frac{2}{H_1}} \cos\left(\frac{n\pi z}{H_1}\right) \quad n = 1, 2, 3, \dots \quad (24)$$

Similarly, in $y > 0$, the h_n and γ_n are as given, but with H_1 replaced by H_2 . From these, it is trivial to determine the matrix elements C_{ij} and G_{ij} analytically. This provides for rapid determination of the scattering coefficients.

3.2.2. Exponential Stratification. We shall also consider an exponential stratification profile, identical to that used in Willmott and Mysak (1980). This comprises a surface mixed layer of constant density ρ_1 , occupying $0 < z < H_3$, above a stratified layer with buoyancy frequency given by

$$N^2(z) = N_0^2 e^{\gamma z}, \quad (25)$$

in the range $-H_1 < z < 0$. This exponential profile may be thought of as a parameterisation of realistic ocean stratification, representing a thermocline at depth H_3 and width of the order $1/\gamma$. In the limit $\gamma \rightarrow 0$ (and $H_3 \simeq 0$) we would expect to recover the results for constant stratification. In the limit $\gamma \rightarrow \infty$, we would expect to recreate the results of the two layer models considered by Wang and Koblinsky (1994). We shall assume throughout that the topography does not penetrate into the mixed layer, i.e. $H_1 > 0$, $H_2 > 0$.

Following Willmott and Mysak (1980), upon making the substitution $s = \exp(\gamma z/2)$ the Sturm-Liouville equation for γ_n , Γ_n becomes

$$\frac{d^2\Gamma_n}{ds^2} - \frac{1}{s} \frac{d\Gamma_n}{ds} + \frac{4N_0^2}{\gamma^2 gh_n} \Gamma_n = 0, \quad -H < z < 0, \quad (26)$$

where $H = H_1, H_2$ depending on the domain. This equation has analytic solutions which may be written in terms of Bessel functions. The baroclinic eigenfunctions ($n = 1, 2, \dots$) are given by

$$\Gamma_n(z) = \begin{cases} 0, & 0 < z < H_3, \\ a_n e^{\gamma z/2} [J_1(\mu_n e^{z/2}) Y_0(\mu_n) - Y_1(\mu_n e^{z/2}) J_0(\mu_n)], & -H < z < 0, \end{cases} \quad (27)$$

where a_n is a normalisation constant, and

$$\mu_n = \sqrt{\frac{4N_0^2}{\gamma^2 g h_n}}. \quad (28)$$

The normalized barotropic eigenfunction is given by

$$\Gamma_0 = \sqrt{\frac{1}{H_1 + H_3}}, \quad -H_1 < z < H_3. \quad (29)$$

Due to the discontinuity in the density gradient, the baroclinic eigenfunctions are similarly discontinuous at $z = 0$, and so rather than the rigid lid condition at $z = H_3$ we have imposed on the solution in equation (27) that $\Gamma'(0) = 0$, to ensure the continuity of the vertical velocity field. The eigenfunctions above satisfy this condition for any value of μ_n and so the eigenvalues must be determined numerically from the bottom boundary condition, $\Gamma'(-H) = 0$, i.e.

$$\mu_n s [J_0(\mu_n s) Y_0(\mu_n s) - Y_0(\mu_n s) J_0(\mu_n)] = 0, \quad \text{at } s = \exp(-\gamma H/2). \quad (30)$$

3.2.3. Layered model. In addition to the continuously stratified model, we shall show results for a two-layer model, such as that considered by Wang and Koblinsky (1994). As shown in Rhines (1977), the stream-function in the upper and lower layer, ψ_1 and ψ_2 , each satisfy the quasi-geostrophic equation

$$\frac{D}{Dt} \left\{ \nabla \cdot \left[\frac{1}{\eta_i} \nabla \psi_i \right] + \frac{f}{\eta_i} \right\} = 0, \quad (31)$$

where D/Dt is the advective derivative and η_i is the perturbed depth of the i th layer. (Further details, and the resulting dispersion relations are given Appendix A.) Since the horizontal velocity field in each layer is depth independent, it is not possible to impose a no-normal-flow condition on the vertical face of the topography. Instead, continuity of the interfacial displacement above the step gives one boundary condition; to obtain the other it is necessary to integrate the linearized governing equation across the step, to obtain a condition for $\psi_{1,2}$ such that the jump in relative vorticity balances the jump in potential vorticity due to the vortex stretching terms at the depth discontinuity. Details of this derivation may be found in Appendix B.

It is not immediately apparent whether this process is justified, since QG theory is valid only in regions in which the bottom topography is slowly varying. In contrast, our continuously stratified model solves the QG equations only in the case of flat bottom, and then applies the correct boundary condition at the depth discontinuity to couple these solutions together.

4. Numerical results

We have now described the method of solution for the scattering by an escarpment, and can employ this for the case of scattering by a ridge of finite thickness; this is achieved

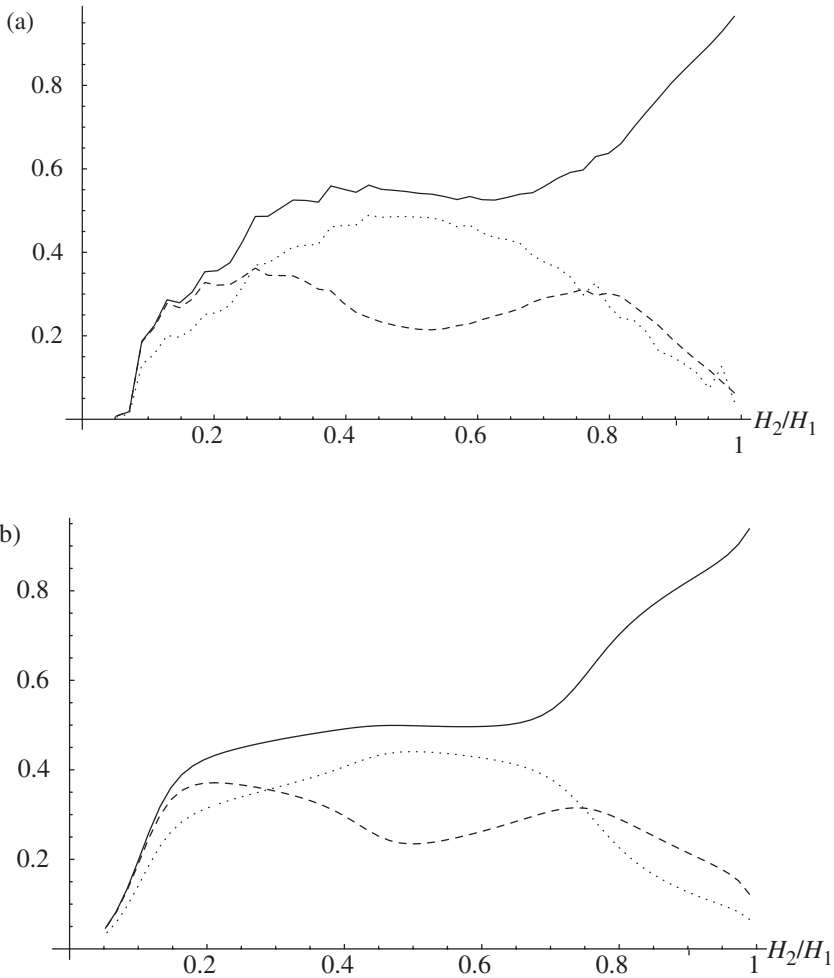


Figure 3. Plot of transmission coefficients for a narrow ridge ($2l = 200$ m) in an ocean with N approximately constant (a) and N constant (b). The solid line shows the first baroclinic mode, the dashed line shows the second baroclinic mode, the dotted line shows the barotropic mode.

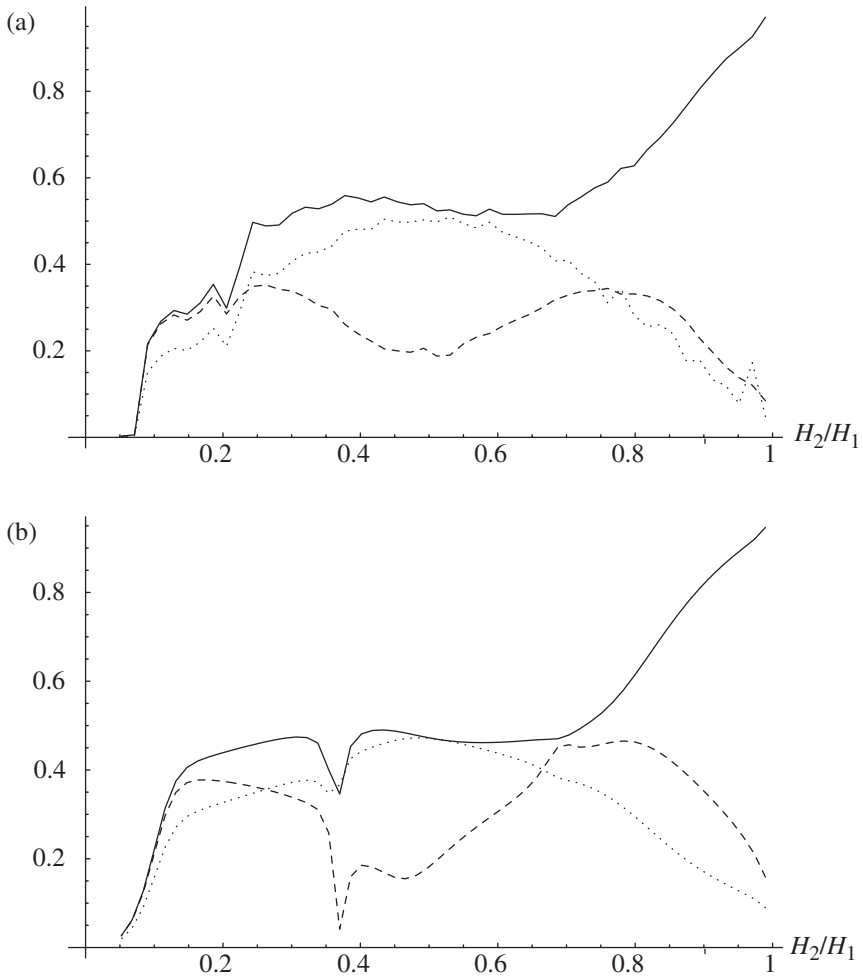


Figure 4. As figure 3 except for a wide ridge ($2l = 200$ km).

by the simultaneous solution of two escarpment problems, at $y = -l$ and $y = +l$. Unless otherwise stated, we shall consider an ocean of depth $H_1 = 4.8$ km, $H_3 = 200$ m, at a latitude of 60°N forced by waves of semi-annual period, $N_0 = 0.02 \text{ s}^{-1}$ and $\theta = 30^\circ$. We use 500 modes for matching.

4.1. Near-linear stratification

To verify the efficacy of the solution procedure, we shall first consider the case where $\gamma = 10^{-5}$, i.e. $\gamma H = 5 \times 10^{-2} \ll 1$. Thus the buoyancy frequency is approximately constant, with its value taken to be $N_0 = 0.02 \text{ s}^{-1}$. In this limit, we expect to recover the results of Owen *et al.* (2002) when the ridge is “narrow”. Figure 3 shows transmission coefficients when the step is narrow, in the sense that its width is very much less than the horizontal decay-scale of the evanescent modes. Here, we consider a ridge of width $2l = 200$ m. Clearly, the solutions for near-constant N are close to those

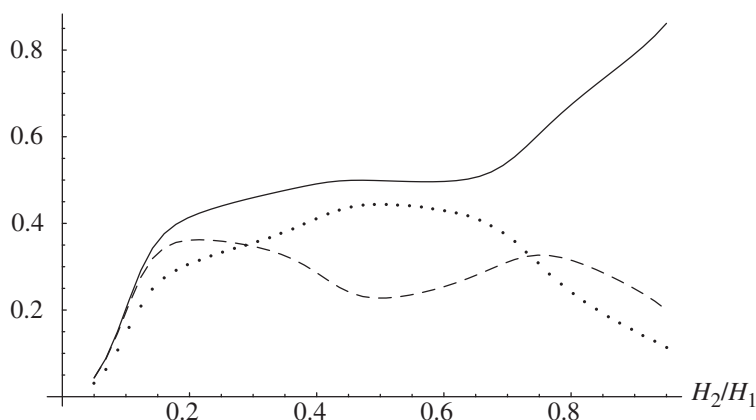


Figure 5. Transmission coefficients for a ridge of infinitesimal width in an ocean with constant N , as discussed in Owen *et al.* (2002). The lines have the same meaning as in figure 3.

for constant N , and comparison with results from Owen *et al.* (2002), reproduced in figure 5, shows that in the limit as the ridge width tends to zero, the results for a ridge of infinitesimal width are recovered.

The effect of a wide ridge (much longer than the decay scale of evanescent modes) is seen in figure 4 (with $2l = 200$ km). Perhaps surprisingly, the results are similar to those for the short ridge, with discrepancies occurring only at values of ridge height for which propagating modes cut off. For example, when $H_2/H_1 \simeq 0.7$ km the equivalent depth, h_3 , above the ridge is such that the roots of the dispersion relation change from real to imaginary. Hence, the number of baroclinic modes that may propagate over the ridge changes from 3 to 2. Similarly, for $H_2 < 0.36$ km there is only a single propagating baroclinic mode. The transition causes the visible cusps in the graphs at these locations, which are more pronounced in the case of the wide ridge. Note that the exact location of this second discrepancy differs between the two graphs in figure 4, due to the differing eigenvalues for the problem as a result of the inclusion of a mixed layer in the exponentially stratified model.

4.2. Realistic stratification

Figure 6 shows the transmission coefficients for the barotropic and sole propagating baroclinic mode in a stratified ocean, with the majority of density variation confined to a thin thermocline below the mixed layer (i.e. $1/\gamma = 300$ m). It can be seen from these results that even for relatively small height topography, there is a large amount of wave energy reflected from the ridge, and appreciable energy conversion between the propagating barotropic and baroclinic modes. This was true for the constant N problem considered previously, but the effect is even more marked for this more realistic stratification. However, after this initial $O(1)$ change in transmission and reflection coefficients, further variation of the ridge height has little effect on the propagation characteristics, for a wide range of H_2/H_1 . There is sharp cusp near $H_2/H_1 = 0.1$, where the final propagating mode cuts off, which is more pronounced for the wider ridge, since weakly evanescent modes are still able to

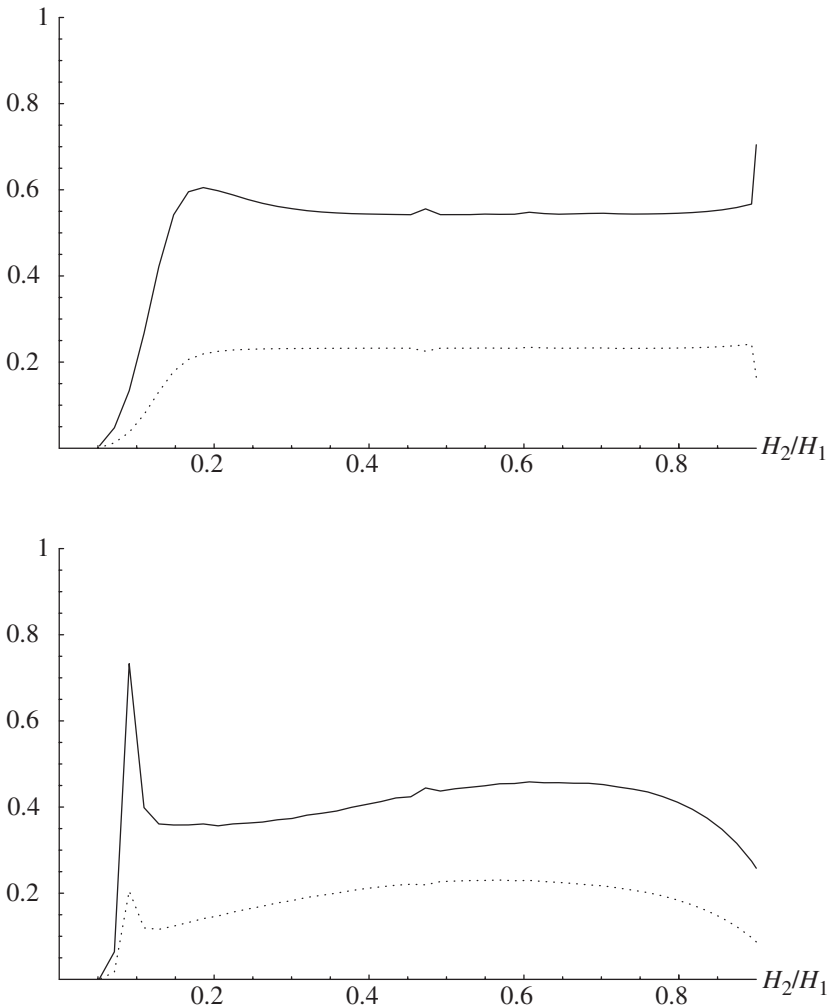


Figure 6. Plot of transmission coefficients against the ratio H_2/H_1 for a narrow (top) and wide (bottom) ridge in an ocean with the variation in N confined to a thermocline of depth 300 m

cross the narrow ridge. After this cusp, transmission is rapidly damped as the ridge reaches the thermocline and the final propagating baroclinic mode is cut off. It would appear, then, that the wave response to abrupt topography is dominated by the physics in the abyssal ocean. In this region, the Brunt-Väisälä frequency is small, so the corresponding periods ($2\pi/N$) have risen from minutes to many hours. Thus, the ratio, f^2/N^2 is $O(1)$, and the local buoyancy parameter

$$S = \frac{N^2}{f^2} H_1^2 K^2, \quad (32)$$

is small, where K^2 is given in equation (36). This results in inhibited vertical velocity near the ocean floor. Physically, the effect of the rotation on the weakly stratified

abyssal ocean is to constrain fluid parcels to near-horizontal flow, and thus prevent the wave energy from passing over the obstacle.

4.3. Layered model

While the layered model attempts to portray the thermocline structure, the physical processes and vertical wave propagation in the abyssal ocean are absent. Combined with the difference between the boundary conditions employed at the depth discontinuity, it is perhaps not surprising that results differ qualitatively between the layered and continuously stratified models. Figure 7 shows the transmission coefficients for

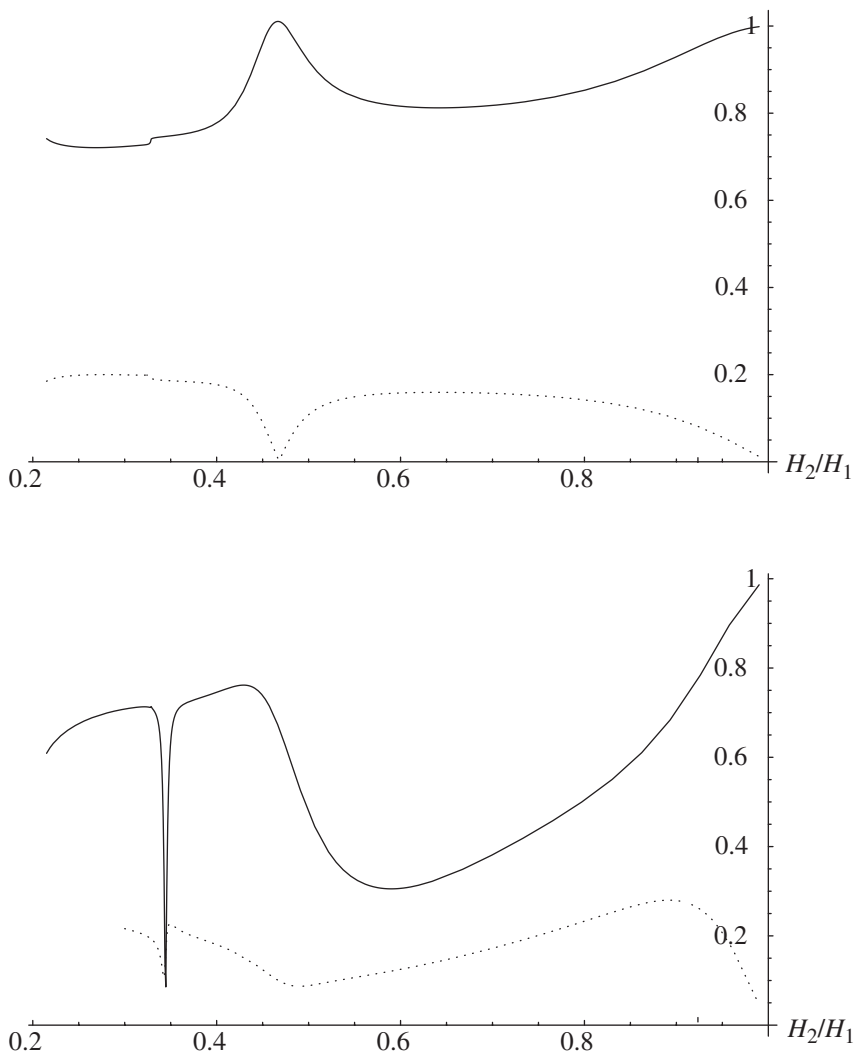


Figure 7. Transmission coefficients for a narrow (top) and wide (bottom) ridge in a two-layer ocean. The solid line denotes the baroclinic mode and the dotted line the barotropic mode.

a two-layer model (which supports only two modes – one baroclinic and one barotropic), with reduced gravity, g' , given by

$$g' = \frac{g\Delta\rho}{\rho_*} = \int_{-H_2}^0 N^2(z)dz, \quad (33)$$

chosen for consistency with figure 6. As previously noted, it is questionable as to whether boundary condition derived from the linearized QG equation is valid for sizeable topography. These results are qualitatively similar to those given in Wang and Koblinsky (1994), although in that paper the authors set the upper and lower layer depths equal, sacrificing oceanographic realism for ease of exposition. However, the results are clearly different from those shown in figure 6; the layered models do not exhibit appreciable reflection for small amplitude topography, and the results are quite distinct in the cases of wide and narrow ridges.

5. Asymptotic solution

As noted above, numerical experiments reveal a qualitative difference between strongly stratified models that approach a two-layer density profile and a two-layer model. The behaviour in the former, where the scattering is dominated by the physical process in the abyssal ocean, leading to considerable scattering even by small topography, might be considered counter-intuitive. However, such phenomena are not unknown in the theory of rotating fluids; for example, in the problem considered by Willmott and Johnson (1995), the topographically supported waves are of great importance in the long timescale geostrophic adjustment. Furthermore, when solving the scattering problem in a strongly stratified ocean, with small amplitude topography ($1 - H_2/H_1 \ll 1$), the partition of the eigenvalues described in section 3.1 results in few eigenvalues near zero (or none at all), leading to solutions which violate the no-normal-flow condition. Given these numerical problems, we shall attempt to verify the above results with a formal solution in the problematic regime using matched asymptotic expansions, (see Crighton *et al.* 1992).

In the manner of Owen *et al.* (2002) we shall consider an ocean with no mixed layer, i.e. $H_3 = 0$. We first apply the carrier-wave transformation,

$$\psi(y, z) = \tilde{\psi}(y, z) \exp(i\lambda y) \quad \text{with} \quad \lambda = -\frac{\beta \sin \theta}{2\omega}, \quad (34)$$

to the Rossby wave equation (4). Suppressing the sinusoidal dependence on x and t , ($\exp(ikx - \omega t)$), we obtain the equation

$$\frac{\partial^2 \tilde{\psi}}{\partial y^2} + \frac{\partial}{\partial z} \left[\frac{f_0^2}{N^2} \frac{\partial \tilde{\psi}}{\partial z} \right] + K^2 \tilde{\psi} = 0, \quad (35)$$

where the wavenumber K is given by

$$K^2 = \left[\frac{\beta^2 \sin^2 \theta}{4\omega^2} + \frac{\beta k \cos \theta}{\omega} - k^2 \right] > 0. \quad (36)$$

Throughout the remainder of this section, we shall suppress the tilde on the transformed potential, $\tilde{\psi}$. To perform the asymptotic expansion we exploit the scale disparity between the wavelength of the propagating waves and the height of the barrier. We exploit this disparity in order to divide the problem geometry into two regimes, each dominated by different physical processes.

5.1. Outer problem

In the outer regime, the ocean physics are governed by the balance between the horizontal wave motion induced by the potential vorticity conservation on the β -plane and the vertical motions supported by the stratification of the lower layer. Defining the $O(1)$ stratification parameter, S_0 , by

$$S_0 = \frac{N_0^2}{f_0^2} H_1^2 K^2 \tag{37}$$

we introduce the dimensionless outer variables

$$\bar{y} = Ky \quad \text{and} \quad \bar{z} = \frac{S_0^{1/2}}{H_1} z, \tag{38}$$

the scaled depth $\bar{H} = S_0^{1/2}$ and the parameter $\bar{\gamma}$ such that $\gamma z = \bar{\gamma} \bar{z}$. In outer variables, equation (35) becomes

$$\frac{\partial^2 \psi}{\partial \bar{y}^2} + \frac{\partial}{\partial \bar{z}} \left[e^{-\bar{\gamma} \bar{z}} \frac{\partial \psi}{\partial \bar{z}} \right] + \psi = 0. \tag{39}$$

We introduce a Green's function, $g(y, z)$, that solves the equation

$$\frac{\partial^2 g}{\partial y^2} + \frac{\partial}{\partial z} \left[e^{-\gamma z} \frac{\partial g}{\partial z} \right] + g = \delta(\bar{y}) \delta(\bar{z} + \bar{H}), \tag{40}$$

and assume that when scaled according to equation (38) the ridge is small, in both horizontal and vertical extent. In this case, we may integrate around the contour $\partial \mathcal{V}$ shown in figure 8 and apply Green's theorem in the plane to obtain the relationship

$$\psi = \int_{\mathcal{V}} \{ \psi \nabla^2 g - g \nabla^2 \psi \} dS = \int_{\partial \mathcal{V}} \left\{ \psi \frac{\partial g}{\partial n} - g \frac{\partial \psi}{\partial n} \right\} dL, \tag{41}$$

where dS and dL are area and line elements respectively and $\partial/\partial n$ denotes the outward normal derivative on $\partial \mathcal{V}$, which encircles the domain \mathcal{V} . From the boundary conditions satisfied by g and ψ , the contributions to the integral on the right hand side of equation (41) from the top and bottom segments vanish and, by symmetry, the integral over the vertical sections yield the incident harmonic wave. Thus, the perturbation to the stream function due to the ridge is given by the integral over the faces of the topography. Since the topography is, by definition, in the inner region, we may

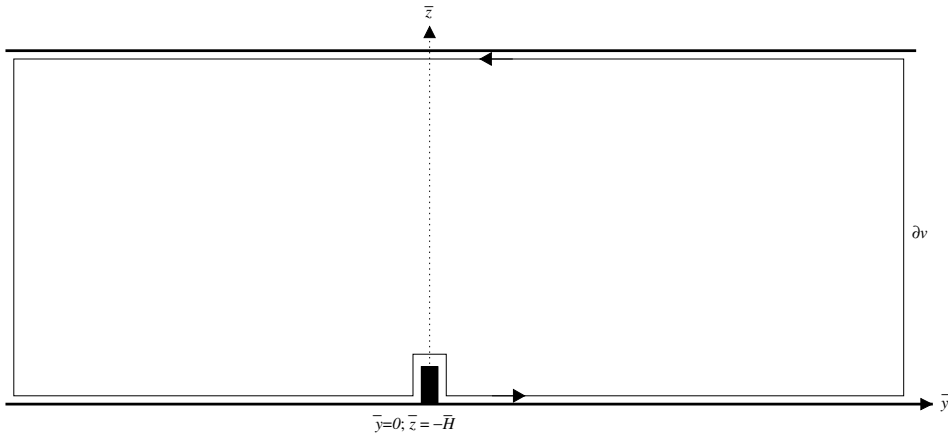


Figure 8. Contour used for the application of Green's theorem.

rewrite this integral in the inner variables and expand as a Taylor series. Considering only the leading order term, and noting that ψ vanishes on the vertical faces and both $\partial\psi/\partial n$ and $\partial g/\partial n$ vanish (to leading order) on the horizontal face, we have

$$\psi^{(o)} \sim g(\bar{y}, \bar{z}) \int_{-H_1}^{-H_2} \left\{ \frac{\partial\psi}{\partial n} \Big|_{y=-l} + \frac{\partial\psi}{\partial n} \Big|_{y=+l} \right\} dz = a_0 g(\bar{y}, \bar{z}), \quad (42)$$

where the superscript on ψ denotes that this is the perturbation to the incident plane wave. Thus, the perturbation is identical to that induced by a line source situated at $(y, z) = (0, -H_1)$ (in physical variables), of as-yet-undetermined source strength, a_0 . The Green's function itself may be found using standard transform techniques. Fourier transforming equation (40) in the y direction, we obtain the ordinary differential equation

$$\frac{d}{d\bar{z}} \left[e^{-\gamma\bar{z}} \frac{d\Psi}{d\bar{z}} \right] + (1 - \alpha^2)\Psi = \delta(\bar{z} + \bar{H}), \quad (43)$$

where $\Psi(\alpha, \bar{z})$ is the transformed potential and α is the transform variable. Making the substitution $s = \exp(\gamma\bar{z}/2)$, this equation may be solved in an identical manner to the Sturm–Liouville equation (26). Imposing the rigid lid and impermeable bottom boundary conditions and inverting the Fourier transform, it may be seen that this Green's function solution may be written

$$\psi^{(o)}(\bar{y}, \bar{z}) = \frac{a_0}{\pi\gamma} \int_{-\infty}^{\infty} \frac{e^{-\alpha\bar{y}} s C_1(t, s)}{t(\alpha) C_0(t, s_*)} d\alpha, \quad (44)$$

where $s_* = \exp(-\gamma\bar{H}/2)$,

$$t^2(\alpha) = \frac{4}{\gamma^2} (1 - \alpha^2), \quad C_1(t, s) = Y_0(t)J_1(ts) - J_0(t)Y_1(ts) \quad \text{and} \\ C_0(t, s) = Y_0(t)J_0(ts) - J_0(t)Y_0(ts). \quad (45)$$

The integration contour in equation (44) passes above those real poles in $-1 \leq \alpha < 0$ and below those in $0 < \alpha \leq 1$ and the superscript on ψ denotes the perturbation to the incident plane wave. As is usual in problems concerning waveguides, it may be shown that the integrand in equation (44) is free of branch cuts in the entire complex plane and hence the scattering coefficients may be determined from the residues at the zeros of $C_0(t, s_*)$, the locations of which correspond to the eigenvalues of the Sturm–Liouville problem solved previously.

5.2. Inner problem

In the inner region, the dominant lengthscale is that of the ridge height, and the surface at $z=0$ is removed to infinity. For simplicity and ease of exposition, we shall assume that the ridge is negligibly thin and its height, $h = H_1 - H_2$, is such that the density is approximately constant and the local stratification parameter, which is $O(1)$ within the thermocline, is exponentially small in the abyssal ocean. We have

$$h \ll \frac{1}{\gamma} \ll H_1 \quad \text{and so} \quad e^{-\gamma z} \simeq e^{-\gamma H_1} = s_*^2 \ll 1. \quad (46)$$

After introducing the scaled inner variables

$$Y = \frac{y}{h} \quad \text{and} \quad Z = \frac{z + H_1}{h}, \quad (47)$$

the governing equation becomes

$$\frac{\partial^2 \psi}{\partial Y^2} + \frac{f_0^2}{N_0^2 s_*^2} \frac{\partial^2 \psi}{\partial Z^2} + \varepsilon^2 \psi = 0, \quad (48)$$

where the small parameter $\varepsilon = Kh$. If we make the convenient substitution $\xi = f_0 Y / N_0 s_*$ then to leading order in ε the equation of motion becomes Laplace's equation and the inner problem is now identical to that solved in Owen *et al.* (2002). Its solution is easily shown to be given by

$$\psi^{(i)}(\xi, Z) = -\Gamma_1(-H_1) + A_0 \operatorname{Re}\{\cosh^{-1}(Z + i\xi)\}, \quad (49)$$

where A_0 is an undetermined constant. The superscript on ψ here indicates that this is the leading order 'inner' solution.

5.3. Matching procedure

To perform the matching, and thereby determine the matching constants a_0 and A_0 we must obtain the far-field form of the inner solution and, conversely, a near-field expansion for the outer solution. It is easily shown from equation (49) that the inner solution may be written

$$\psi^{(i)}(\xi, Z) \sim -\Gamma_1(-H_1) + A_0 \log(2R), \quad (50)$$

where $R = (\xi^2 + Z^2)^{1/2}$. We may find the asymptotic form of the Green's function (outer) solution (44) by examining the integral behaviour as $\bar{x}, \bar{y} \rightarrow 0$, or equivalently as $|\alpha| \rightarrow \infty$. Alternatively we could consider a local analysis in the region of the source; in this region the buoyancy frequency attains its constant abyssal value and we can neglect the effect of the upper surface. Thus, to leading order the Green's solution is the standard one for the Helmholtz equation with point source near a straight barrier with Neumann boundary conditions, that is,

$$\psi^{(o)}(\bar{y}, \bar{z}) \simeq \frac{a_0 s_*}{2i} H_0^{(1)}(\bar{r}) \sim \frac{a_0 s_*}{\pi} \left\{ \log \frac{\bar{r}}{2} + \gamma_e + \frac{\pi}{2i} \right\}, \quad (51)$$

where γ_e is Euler's constant ($\simeq 0.577216$) and

$$\bar{r} = \frac{\varepsilon N_0 s_*}{f_0} R. \quad (52)$$

As noted previously, for realistic ocean stratifications the buoyancy frequency in the abyssal ocean is comparable to the Coriolis parameter and so the dimensionless quantity $N_0 s_* / f_0$ is $O(1)$. Applying the Van-Dyke procedure to match the asymptotic results in equations (50) and (51) we find

$$a_0 = -\frac{\pi}{s_*} \frac{\Gamma_1(-H_1)}{\log(N_0 s_* \varepsilon / 4 f_0) + \gamma_e + \pi / 2i}. \quad (53)$$

To determine the scattering coefficients, we must find the residues at the poles in equation (44). However, for brevity we omit most of these results, which must be calculated numerically, and concern ourselves only with the barotropic mode coefficients, given by the residues at $\alpha = \pm 1$. This will suffice to demonstrate the point in question. The residue of the integral in equation (44) at $\alpha = -1$ can be determined explicitly, and its contribution to the integral is given by

$$-2\pi i \times \frac{a_0}{\pi \bar{y}} \lim_{\alpha \rightarrow -1} \left[(\alpha + 1) \frac{e^{-i\alpha \bar{y}} s \mathcal{C}_1(t, s)}{t(\alpha) \mathcal{C}_0(t, s_*)} \right] = \frac{a_0 e^{i\bar{y}}}{2i \bar{H}}. \quad (54)$$

Substituting from equation (53), the barotropic component of the transmitted wave field is given by

$$T_0 e^{i\bar{y}} \Gamma_0 = \frac{\pi i}{2 s_* \bar{H}} \frac{1}{\log \varepsilon'} [e^{i\bar{y}} \Gamma_1(-H_1)] \quad (55)$$

where $\log \varepsilon' = \log(N_0 s_* \varepsilon / 4 f_0) + \gamma_e + \pi / 2i$. Thus, the transmission coefficient for the barotropic mode is given by

$$T_0 = \frac{\pi i \Gamma_1(-H_1)}{2 s_* \Gamma_0 \bar{H}} \times \frac{1}{\log \varepsilon'}. \quad (56)$$

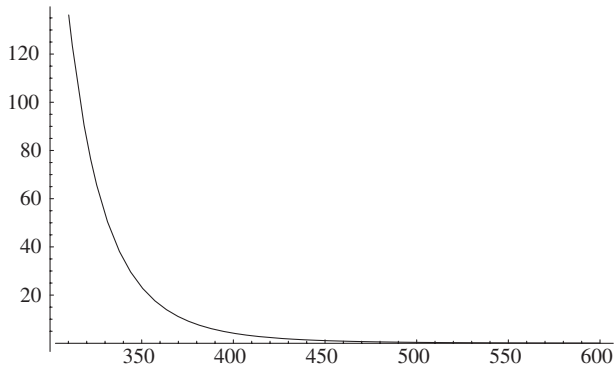


Figure 9. Absolute value of the coefficient of $1/\log \epsilon'$ in the barotropic mode transmission coefficient (56).

It may be seen that as the e-folding scale decreases, the parameter s_* becomes exponentially small and, as shown in figure 9, the perturbation induced by small barriers can become very large. This is entirely consistent with the numerical results obtained previously.

6. Conclusions

Having successfully extended the work carried out previously, several qualitative statements can be made about the factors which are of most importance in the scattering by abrupt topography. The difference between scattering from wide and narrow ridges is due mainly to the influence of the evanescent modes. These modes are topographically trapped near each escarpment, and are felt at the other discontinuity only for narrow ridges. However, it is clear that their influence on the scattering is not marked, having a noticeable effect on the scattering and mode conversion only around ridge heights at which the propagating modes over the ridge cut on and off. The implication, which is borne out both by consideration of the wave field reflected from the far end of the ridge and results obtained for scattering by the escarpment geometry (not presented here), is that the most important factor is the initial scattering by the topography – wave energy which passes onto the ridge is efficiently converted into propagating disturbances on the far side of the topography.

The most important result to note from the present analysis is that scattering characteristics depend crucially on the stratification in the abyssal ocean, as well as the thermocline structure. We have shown that models (such as the layered model studied by Wang and Koblinsky (1994)) which capture neither the essential physics nor accurately represent the boundary conditions, behave qualitatively and quantitatively differently to continuously stratified models. Thus, the application and use of two layer models in place of continuous stratification cannot be recommended in general.

Acknowledgement

This work was supported by institutional Leverhulme Trust research grant #F/130/U.

References

- [1] Chelton, D.B. and Schlax, M.G., Global observations of oceanic Rossby waves. *Science*, 1996, **272**, 234–238.
- [2] Crighton, D.G., Dowling, A.P., Ffowcs Williams, J.E., Heckl, M. and Leppington, F.G., *Modern Methods in Analytical Acoustics. Lecture Notes*, 1992 (Springer-Verlag: London).
- [3] Emery, W.J., Lee, W.G. and Magaard, L., Geographical and seasonal distributions of Brunt-Väisälä frequency and Rossby radii in the North Pacific and North Atlantic. *J. Physical Oceanography*, 1984, **14**(2), 294–317.
- [4] Hill, K.L., Robinson, I.S. and Cipollini, P., Propagation characteristics of extratropical planetary waves observed in the ATSR global sea surface temperature record. *J. Geophysical Research*, 2000, **105**(C9), 21927–21946.
- [5] Owen, G.W., Willmott, A.J., Abrahams, I.D. and Hughes, C.W., On the scattering of baroclinic Rossby waves by a ridge in a continuously stratified ocean. *J. Fluid Mechanics*, 2002, **465**, 131–155.
- [6] Pedlosky, J., *Geophysical Fluid Dynamics*, 1979 (Springer-Verlag: New York).
- [7] Rhines, P.B., The dynamics of unsteady currents. *The Sea*, Vol. 6, pp. 189–318, 1977 (John Wiley and Sons: New York).
- [8] Wang, L.P. and Kobalinsky, C.J., Influence of mid-ocean ridges on Rossby waves. *J. Geophysical Research*, 1994, **99**(C12), 25143–25153.
- [9] Willmott, A.J. and Johnson, E.R., On geostrophic adjustment of a 2-layer, uniformly rotating fluid in the presence of a step escarpment. *J. Marine Research*, 1995, **53**(1), 49–77.
- [10] Willmott, A.J. and Mysak, L.A., Atmospherically forced eddies in the northern Pacific. *J. Physical Oceanography*, 1980, **10**, 1760–1791.

Appendix

A. Eigenvalue equation for a layered model

The governing equations for a two-layer ocean may be derived by linearizing equation (31) in each layer. Denoting the potential in the upper and lower layers by ψ_3 and ψ_1 (for consistency with their undisturbed depths, H_3 and H_1), we obtain the coupled equations

$$\frac{\partial}{\partial t} \left[\nabla_H^2 \psi_3 + \frac{f_0^2}{g'H_3} (\psi_1 - \psi_3) \right] + \beta \frac{\partial \psi_3}{\partial x'} = 0, \quad (\text{A.1})$$

$$\frac{\partial}{\partial t} \left[\nabla_H^2 \psi_1 + \frac{f_0^2}{g'H_1} (\psi_3 - \psi_1) \right] + \beta \frac{\partial \psi_1}{\partial x'} = 0. \quad (\text{A.2})$$

Looking for eigensolutions of the form

$$\begin{pmatrix} \psi_3 \\ \psi_1 \end{pmatrix} = e^{ikx' + iy'y' - i\omega t} \begin{pmatrix} C_3 \\ C_1 \end{pmatrix}, \quad (\text{A.3})$$

where C_3 and C_1 are unknown constants. Thus, we obtain the eigenvalue equation

$$\left(\omega + \frac{k\beta}{k^2 + l^2} \right) \left(\omega + \frac{k\beta}{k^2 + l^2 + F_1 + F_3} \right) = 0, \quad (\text{A.4})$$

where $F_i = f_0^2/g'H_i$. The first and second roots correspond to the barotropic and baroclinic modes and their associated eigenvectors are, respectively,

$$\begin{pmatrix} 1 \\ 1 \end{pmatrix} \quad \text{and} \quad \begin{pmatrix} 1 \\ -H_3/H_1 \end{pmatrix}. \quad (\text{A.5})$$

B. Solution of layered model

At the escarpment we must consider the governing equation (31), explicitly including the derivatives of the depth discontinuity as generalized functions, i.e. in the lower layer the undisturbed fluid depth is given by

$$h(y) = \begin{cases} H_1, & y < 0, \\ H_2, & y > 0, \end{cases} \quad (\text{B.1})$$

and

$$h'(y) = (H_2 - H_1)\delta(y). \quad (\text{B.2})$$

Then integrating equation (31) in the lower layer over a small interval in y containing the escarpment we obtain the jump condition

$$\left[H \frac{\partial^2 \psi_1}{\partial y \partial t} \right]_{y=0-}^{y=0+} = (H_2 - H_1)ikf_0\psi_1 \quad (\text{B.3})$$

which shows the jump in relative vorticity required to balance the change in the background PV due to the depth discontinuity. Imposing the continuity of the interfacial displacements in both layers implies that ψ_1 , ψ_3 and $\partial\psi_3/\partial y$ are all continuous, and these four conditions are sufficient to find the four unknown scattering coefficients, in a manner similar to that described by Wang and Koblinsky (1994).